**Annales
Geophysicae**

Aurora and open magnetic flux during isolated substorms, sawteeth, and SMC events

A. D. DeJong[1], X. Cai[1], R. C. Clauer[1], and J. F. Spann[2]

[1]Department Atmospheric Oceanic and Space Sciences, University of Michigan, Ann Arbor, MI, USA
[2]NASA Marshall Space Flight Center, Huntsville, AL, USA

Abstract. Using Polar UVI LBHl and IMAGE FUV WIC data, we have compared the auroral signatures and polar cap open flux for isolated substorms, sawteeth oscillations, and steady magnetospheric convection (SMC) events. First, a case study of each event type is performed, comparing auroral signatures and open magnetic fluxes to one another. The latitude location of the auroral oval is similar during isolated substorms and SMC events. The auroral intensity during SMC events is similar to that observed during the expansion phase of an isolated substorm. Examination of an individual sawtooth shows that the auroral intensity is much greater than the SMC or isolated substorm events and the auroral oval is displaced equatorward making a larger polar cap. The temporal variations observed during the individual sawtooth are similar to that observed during the isolated substorm, and while the change in polar cap flux measured during the sawtooth is larger, the percent change in flux is similar to that measured during the isolated substorm. These results are confirmed by a statistical analysis of events within these three classes. The results show that the auroral oval measured during individual sawteeth contains a polar cap with, on average, 150% more magnetic flux than the oval measured during isolated substorms or during SMC events. However, both isolated substorms and sawteeth show a 30% decrease in polar cap magnetic flux during the dipolarization (expansion) phase.

Keywords. Magnetospheric physics (Auroral phenomena; Storms and substorms)

1 Introduction

While auroral substorm signatures and open magnetic flux in the polar cap, as seen by Polar UVI and IMAGE FUV, have

Correspondence to: A. D. DeJong
(dejonga@umich.edu)

been studied in the past (Brittnacher et al., 1999; Perraut et al., 2003; Milan et al., 2003) and references there in, sawtooth oscillations (Henderson et al., 2006) and steady magnetospheric convection (SMC) events (DeJong and Clauer, 2005) have had limited discussion. However, all three classes of events should be studied in parallel due to the ambiguous distinctions between them. For instance, during SMCs there can be pseudo breakups that some consider to be small substorms, while others do not. Also, some postulate that individual sawteeth in a sawtooth interval are just large substorms. Thus, we intend to examine the similarities and differences in the auroral signatures and open magnetic flux in the polar cap, as determined using global auroral imaging, for these three classes of events.

The study is broken up into two parts. The first part presents a case study for each type of event. For ease of comparison, only IMAGE Far Ultraviolet imager (FUV) data is used in this section. The events were chosen for good imaging coverage and limited dayglow. The second part presents a limited statistical study of the polar cap open flux (F_{pc}) for the different types of events. In order to maximize the amount of data, we use both IMAGE FUV and Polar Ultraviolet Imager (UVI). From FUV, we use the Wideband Imaging Camera (WIC) and from UVI we use Lyman-Birge-Hopfield long (LBHl). This part of the study includes events from all seasons, since we have methods of removing dayglow, based on Immel et al. (2000), that allow us to identify the dayside boundary during summer, spring, and fall events.

2 Data and methodology

Figure 1 illustrates how a keogram is created from auroral images for an isolated substorm on 4 January 2001. The upper images are in Apex magnetic coordinates, with the magnetic north pole in the middle of the image at 90 degrees latitude, noon at the top and midnight on the bottom. The
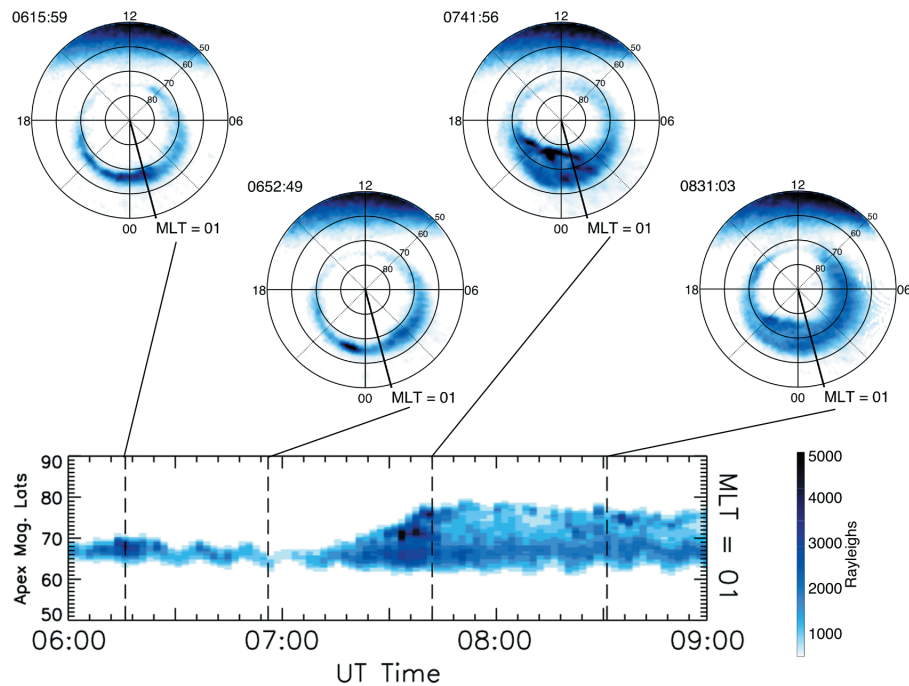
Fig. 1. An example of how a keogram is made using data from the isolated substorm on 4 January 2001. Top shows images from IMAGE FUV WIC in apex magnetic latitude with noon at the top and midnight at the bottom. To make a keogram a slice is taken (01:00 MLT) and then plotted vs. universal time. The color show the intensity of the aurora in Raylieghs.
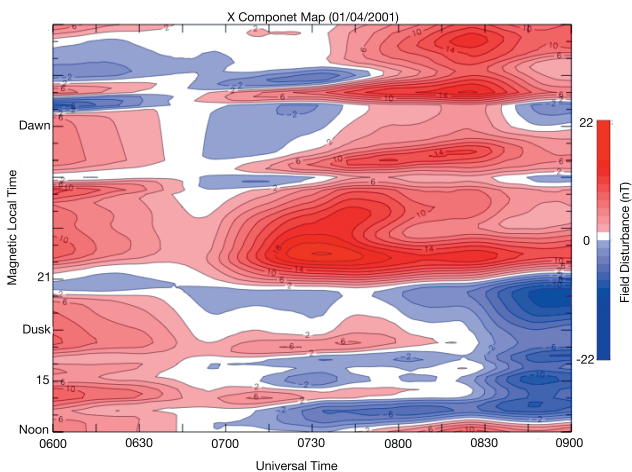

Fig. 2. An MLT-UT map of mid-latitude magnetic perturbations for the isolated substorm on 4 January 2001.

keogram on the bottom is created by taking a slice of the aurora at a chosen Magnetic Local Time, or MLT (01:00 MLT in Fig. 1) and then plotting it against universal time. The color shows the auroral intensity in Rayleighs while the y-axis is Apex magnetic latitude. The keogram starts at 50 apex magnetic latitude at the bottom and goes to 90, or the magnetic north pole, at the top. This configuration allows us to

see the poleward and equatorward movement of the aurora at a specific MLT. However, a keogram at only one MLT conveys a limited amount of information. For example, the auroral onset of the substorm can be seen in the auroral image taken at 06:52 UT at about 22:00 MLT, but since the keogram only shows 01:00 MLT it appears that the onset would be about 10 min later. For this reason, we show keograms for each event at intervals of 02:00 MLT, spanning from 18:00 to 06:00 MLT and going through midnight. This allows us to see the movement of the aurora both in magnetic latitude and magnetic local time (MLT).

When the interplanetary magnetic field (IMF) is oriented southward (B_z negative) reconnection occurs on the dayside of the magnetosphere. This creates magnetic field lines that are open to the solar wind. The edge of the open field lines maps to the poleward boundary of the auroral oval. Thus, the field lines located polarward of the boundary are open and those equatorward are closed. So, if the open-closed boundary can be measured the amount of magnetic flux open to the solar wind can be calculated. We also know that the dayside auroral oval maps to the cusp region whereas the night side maps to the plasma sheet. Therefor, variations in the dayside or night side aurora represent changes in the dayside or night side merging (reconnection) rates. If the merging or reconnection rates on the dayside and night side are balanced then the polar cap and the amount of open magnetic flux in the magnetosphere should remain steady. If the dayside merging
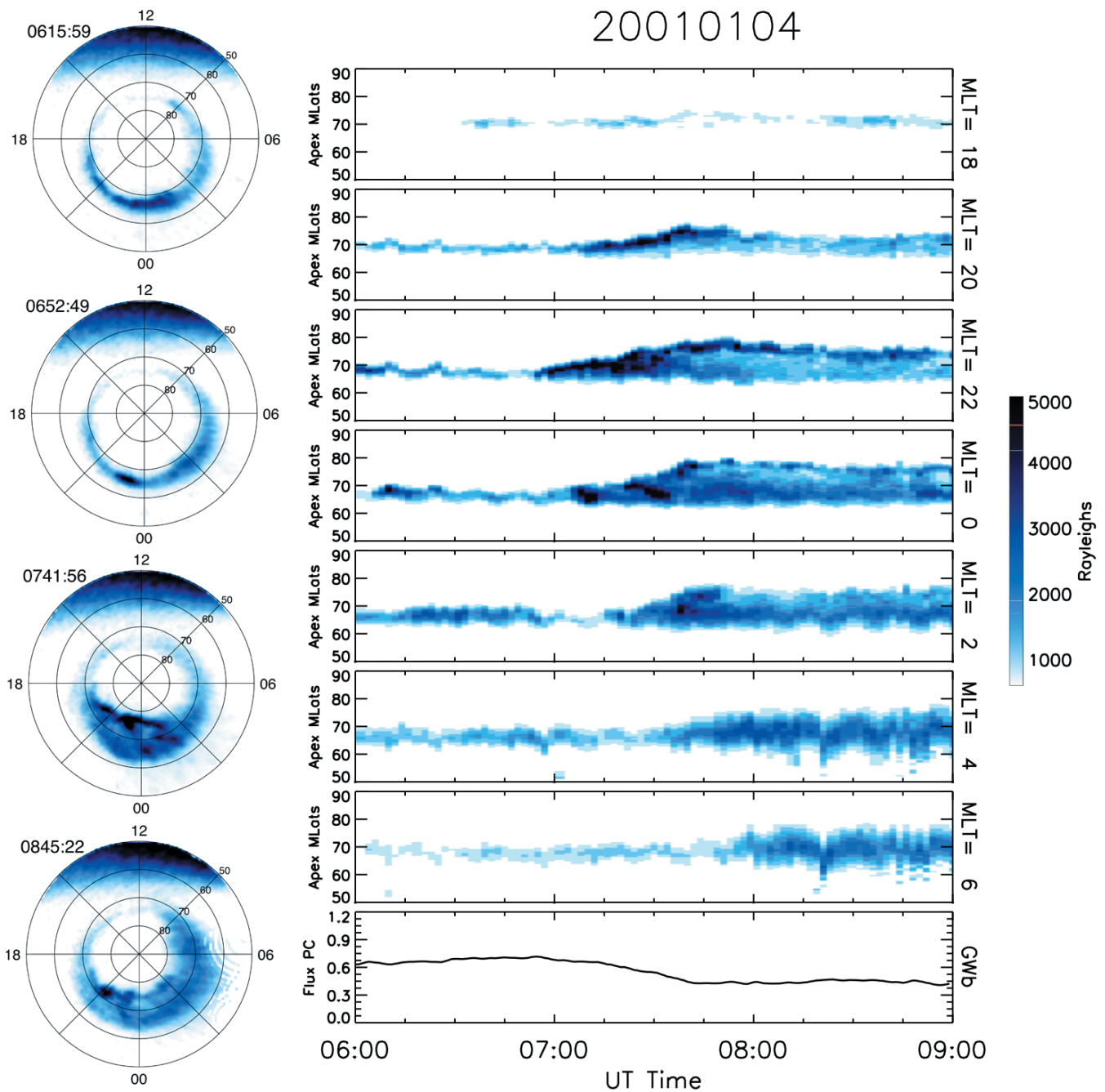
Fig. 3. A stack plot of keograms for the isolated substorm on 4 January 2001. The polar cap open magnetic flux is plotted at the bottom. For reference, there are images of the aurora through out the period shown. The color indicates intensity of the aurora in Rayleighs.

rate is larger than the night side the polar cap will expand, if the night side rate is larger than the dayside the polar cap will contract. Thus, changes in amount of open magnetic flux can inform us about the dayside and night side merging rates.

In order to approximate the amount of magnetic open flux being stored or released, first, we estimate the open-closed boundary for all of the events. According to Baker et al.

(2000), a cutoff intensity of 4.3 photons/cm^2/s gives a good approximation for the open-closed field line boundary when using Polar UVI LBHl data. However, because IMAGE FUV WIC data is in Rayleighs, the Polar UVI data is converted into Rayleighs, resulting in a new cutoff at approximately 130 Rayleighs. Because WIC observes a broader spectrum than LBHl, the images tend to be brighter, causing
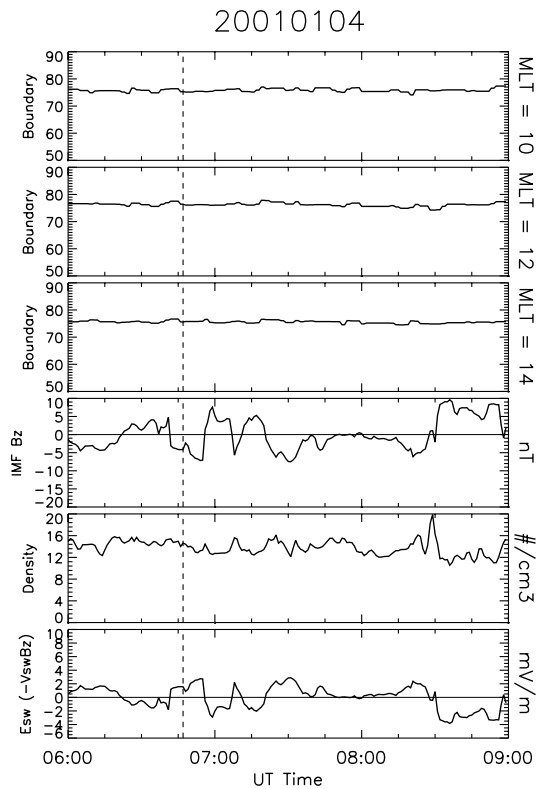
Fig. 4. A stack plot of the dayside boundaries for the isolated substorm on 4 January 2001. **(a)** The magnetic latitude of boundary at 10:00 MLT. **(b)** Magnetic latitude of the boundary at Noon. **(c)** Magnetic latitude of the boundary at 14:00 MLT. **(d)**. IMF B_z (nT) **(e)** Solar wind proton density (number/cm^3) **(f)** The electric field (mV/m) of the solar wind calculated using the solar wind velocity and B_z. The vertical line represent the onset of the expansion phase of the substorm as seen in ground based magnetometer data.

the expected cutoff to be higher. In order to find the FUV boundary, we compared boundaries for events where there are both FUV and UVI data. We found the cutoff for FUV WIC to be about 800 Rayleighs. However, Baker et al. (2000) also found that, during stronger events the more intense aurora calls for higher cut off. This is taken into consideration for both data sets. Once the boundaries are found the amount of open magnetic flux in the polar cap is calculated. This is done by multiplying the integrated area (A_{pc}) by the magnetic field strength in the ionosphere (B_I) (Cowley and Lockwood, 1992; Siscoe and Huang, 1985) using the International Geomagnetic Reference Field (IGRF). Although the auroral boundaries are not exactly the open-closed boundary they are a good approximation and any changes in the auroral boundary should coincide with a similar change in the open-closed boundary. Since we are more interested in the change in the amount of open magnetic flux this a very good representation of the changes we are looking for.
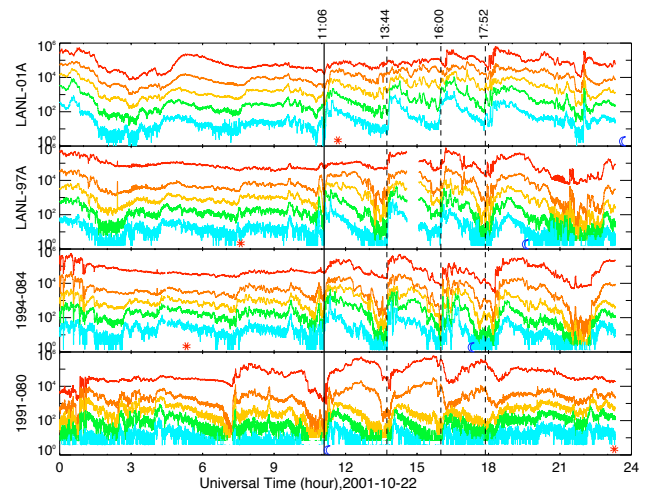

Fig. 5. Plot of LANL SOPA proton data for the sawtooth event on 22 October 2001. The vertical lines illustrate the onset times of the individual teeth.

3 Case studies

3.1 Isolated substorm

In order too identify an event as a substorm, we require a clear mid-latitude positive bay, indicating a substorm current wedge, in mid-latitude magnetometer data (Clauer and McPherron, 1974). The onset of the expansion phase occurs when the first magnetometer starts to see the positive bay. For better visualization, the magnetometer data has been used to create a Magnetic Local Time – Universal Time (MLT-UT) map (Clauer and McPherron, 1974). Figure 2 illustrates an MLT-UT map for the substorm that occurred on 4 January 2001 at 06:47 UT. The red represents a positive change in the data where the blue is a decrease in the data. The local time disturbance measured at the onset set time has been subtracted from all subsequent profiles to provide a better characterization of the substorm and to enable better comparison with other events. While the magnetometer data shows the expansion phase onset at 06:47 UT, as represented by the large red structure that starts at 06:47 UT and spans 21:00 to 03:00 MLT, it does not appear in the FUV images until 06:52 UT. We find a similar shift of onset times in many of our substorms, so for consistency we use the ground magnetometer data alone to determine the onset times.

Figure 3 shows a stack plot of keograms with the F_{pc} plotted at the bottom. For reference, 4 images of the aurora throughout the period are shown on the left. Although others (Brittnacher et al., 1999; Milan et al., 2003) have examined substorms in this fashion, we feel it necessary to have a typical isolated substorm in this study for comparison. The keograms in Fig. 3 go from approximately 1 h before expansion phase onset to 2 h after. The aurora is fairly quiescent
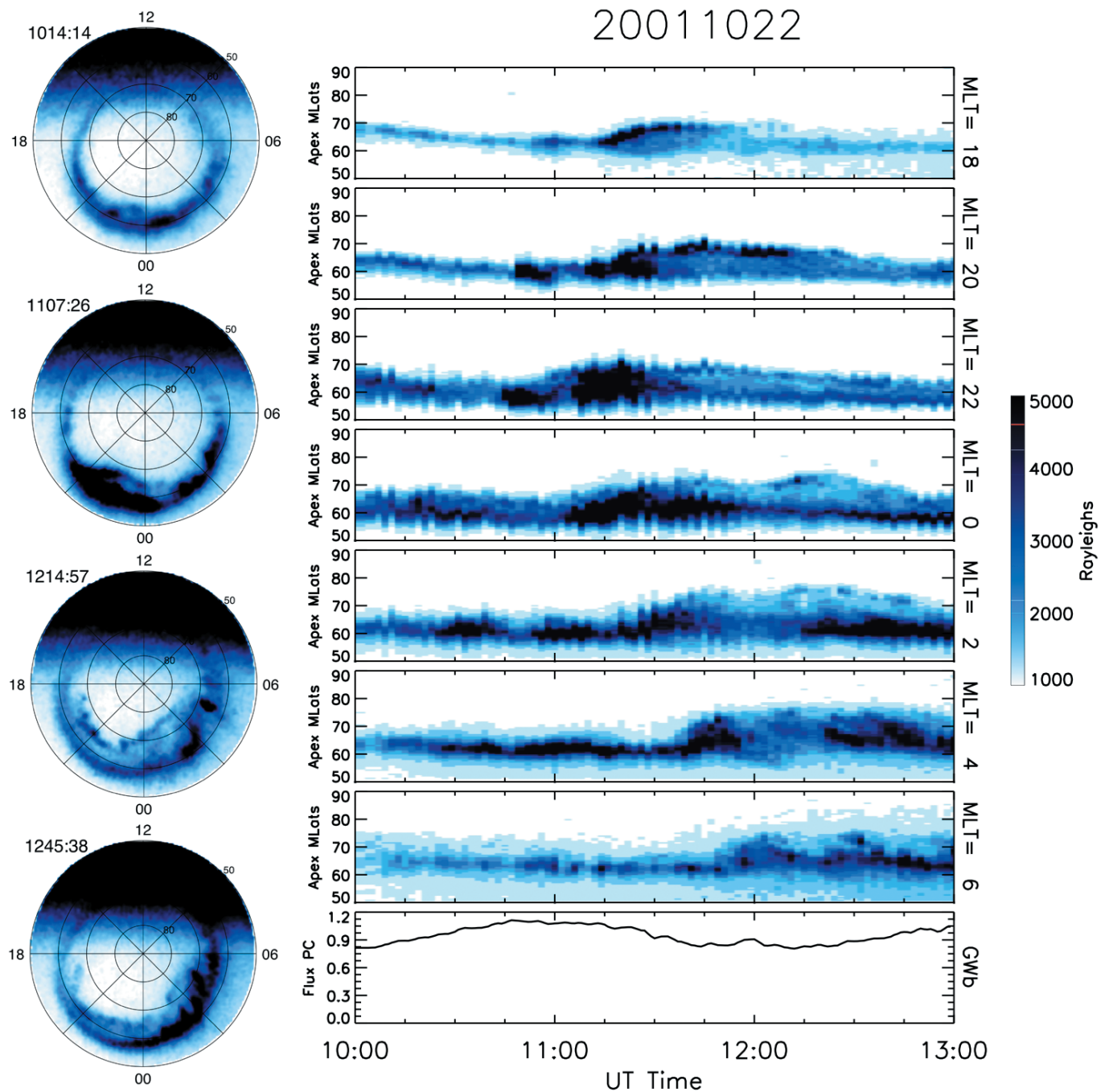
Fig. 6. A stack plot of keograms for the individual sawtooth at 11:06 on 22 October 2001. The set up is the same as Fig. 3.

before the onset and the onset is first seen at 22:00 MLT at 06:52 UT. The substorm then spreads out toward dawn and midnight. Although the substorm is stronger (more intense) on the dusk side, it extends over a greater MLT range on the dawn side. The intensity of the aurora reaches 6000 Rayleighs during the expansion phase and then weakens during the recovery phase. From the keograms, it can also be seen that the intensifications occur more poleward (top of the keogram) at 20:00, 22:00 and 00:00 MLT.

The amount of open polar cap flux in Giga-Webers is plotted on the bottom of Fig. 3. The F_{pc} increases slightly as magnetic flux builds up in the tail, due to an increase in dayside merging, until it reaches a maximum of 0.72 GWb 10 min after onset of the expansion phase. Then, it decreases
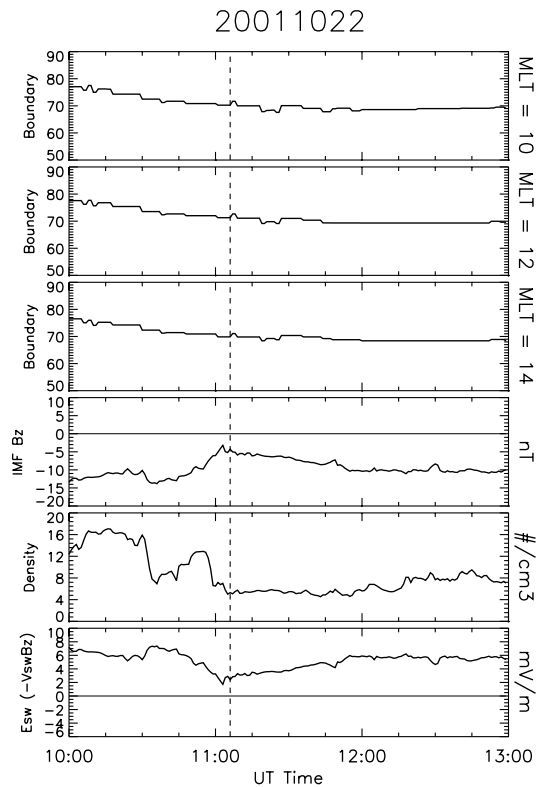
Fig. 7. A stack plot of the dayside boundaries for the individual sawtooth on 22 October 2001. The set up is the same as Fig. 4. The vertical line shows the onset of the injection as measured from geosynchronous satellites.

as magnetic flux is released from the tail during dipolarization, which is caused an increase in the night side merging rate. The open flux continues to decrease until 07:47 UT when it reaches a minimum of 0.42 GWb after which it becomes steady. Thus, the total amount of flux released from the magnetosphere during this substorm is 0.30 GWb which is 42% of the maximum amount of flux.

Figure 4 is stack plot of the magnetic latitude of the dayside boundary along with a few solar wind/IMF parameters, the vertical line is the onset time of the substorm from ground based magnetometer data. The purpose of showing only the boundary location and not keogram lies in our dayglow removal process. The dayside can be clearly seen in individual images of the auroral, but our dayglow removal creates a dark line across the terminator, thus when a keogram is created it is difficult to distinguish between the terminator and the dayside boundary. Since our other two cases studies here occur during October the dayside boundary and the terminator are co-insident at many times. So for consistency we have chosen just to plot the dayside boundary. The interplanetary magnetic field (IMF) and solar wind parameters have been propagated to Earth using the Weimer et al. (2002, 2003,

2004) psuedo-minimum variance technique. The propagation is accurate to approximate 6 min, thus onsets and triggers may not occur at the exact same time. The solar wind density and IMF B_z are plotted due to their role in as a possible trigger for a substorm onset. And E_{sw} is shown since it the major solar wind/IMF component for dayside reconnection (Milan, 2004; Milan et al., 2006). Note that when E_{sw} is positive there is dayside reconnection since B_z is negative. The solar wind/IMF parameters are not very steady and it is difficult to say if there is trigger for the onset of this substorm. However, we could be missing the exact trigger since the propagation time could be a little offset. It is interesting to note that even though the E_{sw} fluctuates from positive to negative during this time it seems to have little effect on the dayside boundary location.

3.2 Individual sawtooth

Sawtooth oscillations are so named because of their appearance in the Los Alamos National Laboratory (LANL) Synchronous Orbit Particle Analyzer (SOPA) proton particle flux data. The particle injections, which have a sawtooth like shape, are seen globally and have a periodicity of 2–4 h.

Although most studies of sawtooth oscillations have included the entire event, which covers many injections, we will concentrate on only one injection as part of our single event analysis. We use the injection at 11:06 UT on 22 October 2001. The sawtooth event is shown in its entirety in Fig. 5, which is a plot of the LANL SOPA proton data at geosynchronous orbit. It is the first injection in this series. This injection was chosen because the aurora imaging data covers the entire injection and there is little dayglow.

The onsets for all of the injections are determined by LANL geosynchronous SOPA proton data. We define the onset with the same criteria in Cai et al. (2006a). Due to the auroral activity before the each injection, it is difficult to see an exact onset in the auroral data. Thus, it is hard to quantify any time delay in the onsets.

Figure 6 uses the same format as Fig. 3. The images on the left of the figure do not have dayglow removed so that the night side aurora can be better seen. There is also no dayglow removal for the keograms, as they are all night side MLTs. The lack of dayglow removal also allows for a better comparison between the intensities of the events. However, dayglow had to be remove in order to measure the dayside boundary to obtain the polar cap flux (F_{pc}).

In comparing Figs. 6 and 3 we can see that the sawtooth is much more intense than the isolated substorm. There is also more auroral activity before the onset. One of the major differences is the extent of the auroral movement in MLT. The isolated substorm studied here is concentrated on the dawn side, whereas the sawtooth extends to 06:00 and 18:00 MLT and beyond. In general isolated substorms are more localized in magnetic local time than individual sawteeth. The maximum intensity of the aurora for the sawtooth is about 15 000
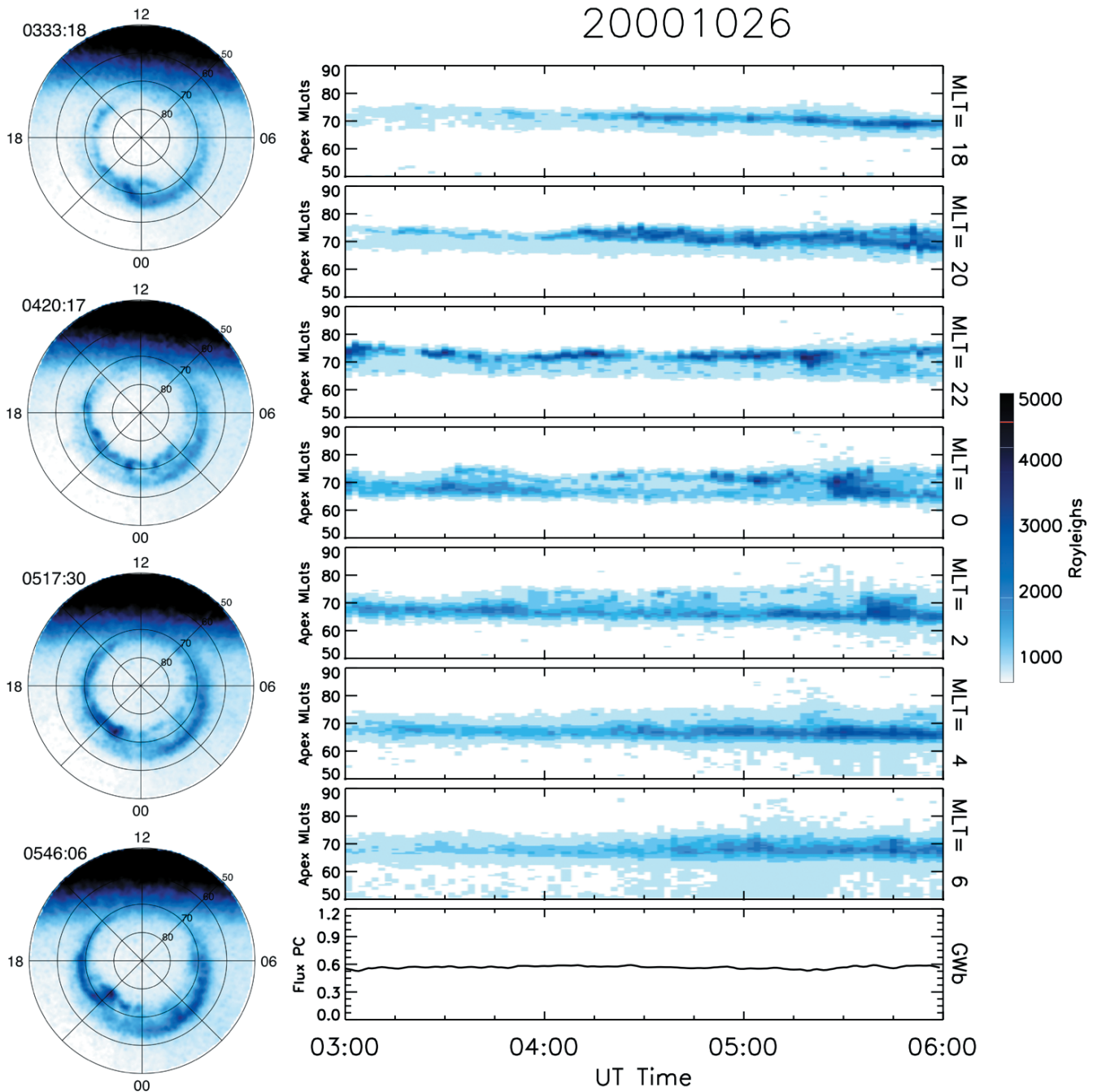
Fig. 8. A stack plot of keograms for the SMC on 26 October 2000. Set up is the same as Fig. 3.

Rayleighs (15 kR) – more than 2 times as intense as the substorm. The intensifications also appear to be more equatorward in 22:00–06:00 MLT keograms, with some brightening poleward in 18:00 and 20:00 MLT keograms. This appears to be part of the double oval discussed in the Henderson et al. (2006) study of the event on 18 April 2002. Also, the sawtooth aurora extends more equatorward than the substorm. The substorm goes no lower than 65 magnetic latitude, whereas the sawtooth extends to 55 magnetic latitude. We found similar intensification patterns and low-latitude boundaries for most of the sawtooth events. This may indicate that sawtooth oscillations may move further into the inner magnetosphere than isolated substorms.

The F_{pc} in Fig. 6 has the same y-axis scale as Fig. 3, making it easier to see that the sawtooth stores and releases much more magnetic flux than the isolated substorm. Also, the
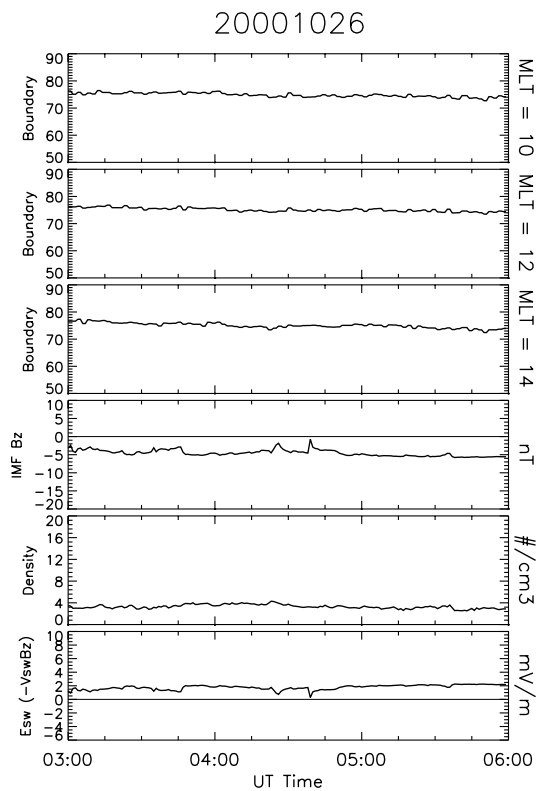
Fig. 9. A stack plot of the dayside boundaries for the SMC on 26 October 2006. The set up is the same as Fig. 4.

"growth" phase or stretching phase is more prevalent as the amount of open flux grows from 0.78 to 1.115 GWb. After the onset, the flux is released just as in the isolated substorm. The minimum amount of F_{pc} is 0.82 GWb which reached approximately 50 min after onset. Thus, 0.29 GWb are released from the tail which is 26% of the maximum flux stored during the event. The sawtooth shows somewhat more recovery of the F_{pc} than the isolated substorm, however it is more complex since the recovery phase and the growth phase of the following oscillation, onset of 13:44 UT, develop simultaneously. This is where it becomes difficult to compare isolated substorms and sawtooth oscillations. In the future, it may be better to look at substorms that occur during a magnetic storm. However, these are harder to determine due to the large levels of activity in the data.

The dayside boundary of the sawtooth is plotted on Fig. 7, which is set up just like Fig. 4. Unlike the isolated substorm the dayside contributes to the storage of open flux in the magnetosphere for this sawtooth. This represented by the equatorward movement of the boundary during the "growth" phase of the sawtooth. The solar wind/IMF data show that the onset was probably triggered by the northward turning that peaks just before onset. Also the E_{sw} reaches a minimum at this point which may have caused a small enough

reconnection line on the dayside that nightside responded by reconnecting and triggering the onset.

3.3 Steady magnetospheric convection event

For comparison we included steady magnetospheric convection events that appear to have pseudo breakups in the auroral signatures. All SMCs are determined using the methodology set forth in DeJong and Clauer (2005), which states that the PC area must be steady for at least 3 h, AE must be greater than 200 nT, and there are no substorm signatures in other data (AE, AL, LANL SOPA, and magnetometer). Because most SMCs start with a substorm (DeJong and Clauer, 2005) and we do not include recovery phases, onset is chosen to be when the PC area becomes steady or at least 1 h after the initial substorm expansion phase onset. Figure 8 shows the first 3 h of the SMC that occurs on 26 October 2000. Only 3 h are used in this study since we used 3 h for the substorm and sawtooth studies. Also, the minimum time requirement for our SMCs is 3 h.

During SMCs the dayside and night side merging or reconnection rates should balance (DeJong and Clauer, 2005). If this holds then the aurora and amount of open flux in the magnetosphere should remain fairly steady. This can be seen in Fig. 8 (same format as Figs. 3 and 6) in that the F_{pc} and the extent of the aurora, both poleward and equatorward, are nearly constant. However, there are fluctuations in the brightness of the aurora. At about 05:15 UT, there appears to be a brightening at 22:00 MLT which seems to move toward dawn. However, there is no poleward movement in the boundary associated with the brightening, and it only lasts for about 20 min. Thus, we consider this to a pseudo breakup not a substorm (Koskinen et al., 1993) and (Fillingim et al., 2000). We see pseudo breakups in many of our SMCs, as did Sergeev et al. (1996); Yahnin et al. (1994), although they did not call them as such. This indicates that the magnetosphere may be considered steady on a large scale but not as steady on a smaller scale.

The dayside boundary and solar wind/IMF parameters (as seen in Fig. 9) are what one would expect during an SMC (O'Brien et al., 2002). The dayside boundary is steady the entire 3 h interval and IMF B_z, solar wind density and E_{sw} are all moderate yet steady.

3.4 Discussion of casestudies

With respect to the auroral intensity and extent in magnetic latitude (65 mag. lat.) the isolated substorm's expansion phase more closely resembles the SMCs. But this is where the similarities end, during the SMC the dayside and night side merging rates are balanced, this is not the case for the substorm. The F_{pc} trends for the substorm follows the same pattern as the sawtooth. They both have a loading and unloading of the F_{pc} thus both start with a larger dayside reconnection rate which then transitions to a larger night side
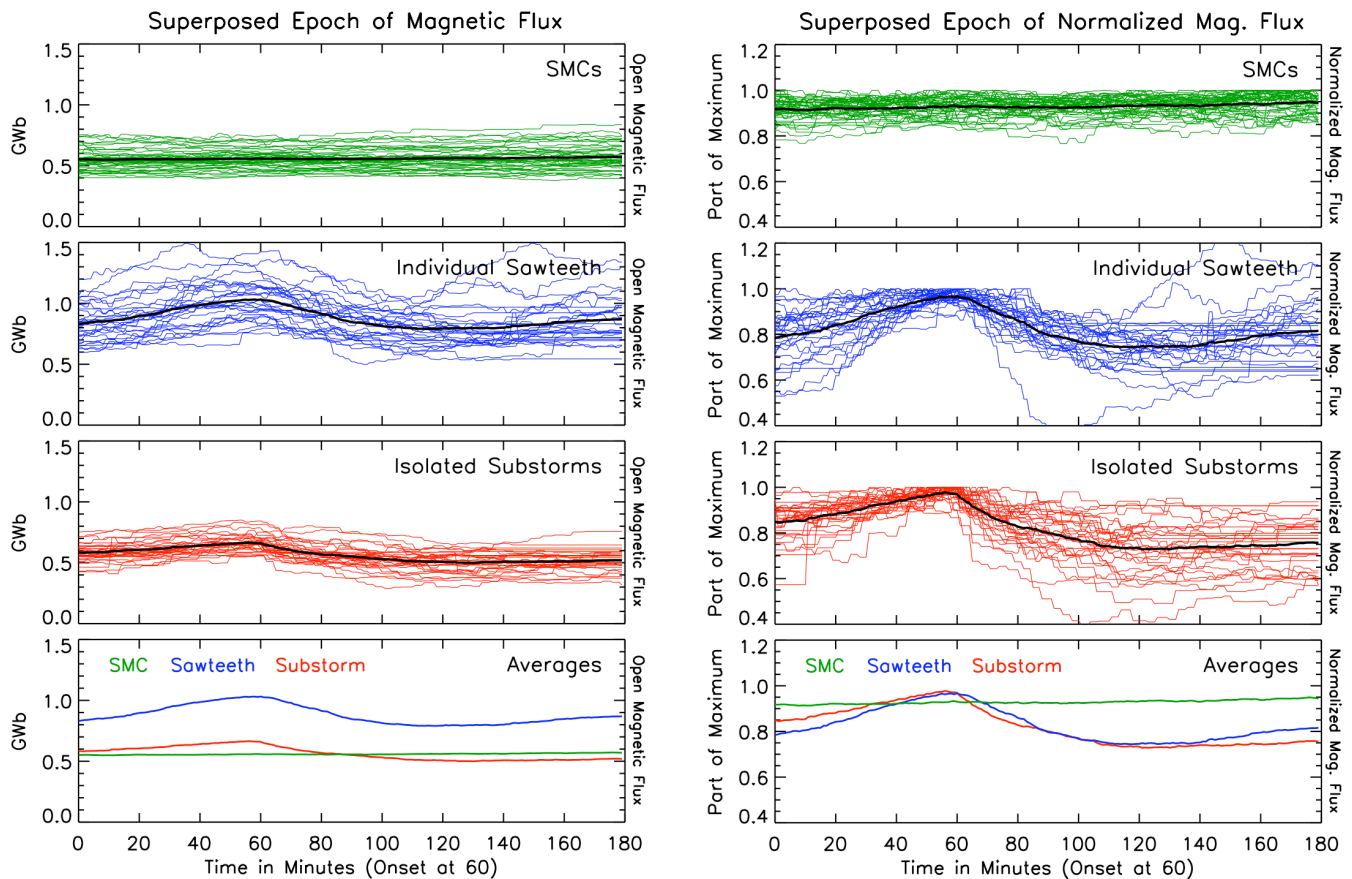
Fig. 10. Superposed epochs of the polar cap open flux for SMCs, isolated substorms and individual sawteeth. The average of are replotted on the bottom. Left is the actual F_{pc} in gigawebers and right is the F_{pc} normalized by the maximum area for the time interval.

reconnection rate after onset. Although the F_{pc} variations during the substorm are smaller than during the sawtooth, the amount of flux released from the tail is approximately 0.30 GWb for both. However, if we look at the percentage of the total this represents, then the substorm releases 42% of the stored flux whereas the sawtooth releases only 26%.

4 Statistical study

In order to better characterize the classes of events described above and to determine the amount of open flux variations during the storage (loading) and release (unloading) portions of the the events, we have conducted a statistical investigation of the F_{pc}. In this portion of the study we used 29 individual sawteeth, 31 isolated substorms, and 45 SMCs (See Appendix for a full lists of events). As stated previously both IMAGE FUV WIC and Polar UVI LBHl data were used in the analysis for all types of events. The top three plots of Fig. 10 are superposed epochs of all the F_{pc} for SMCs (green), individual sawteeth (blue), isolated substorms (red), with the averages over plotted in black. The averages are then replotted at the bottom for a better comparison. Substorms

and sawteeth events are plotted from exactly 1 h before onset, so onset of the event is at 60 min.

The left plot on Fig. 10 is a superposed epoch of the actual values of the F_{pc}. As expected, the SMCs are very steady, while the substorms and sawteeth show growth, expansion and recovery phases. It can be seen that the average of sawteeth F_{pc} is much larger than that of isolated substorms. It appears that on average sawtooth oscillations have a F_{pc} that is 150% as large as isolated substorms, yet the patterns of loading and unloading with respect on the onset time (60 min) are very similar. In order to study the loading and unloading processes more closely the fluxes have been normalized and plotted on the right of Fig. 10. The normalization process was done by dividing by the largest F_{pc} for each event. The SMC patterns are very steady with the smallest F_{pc} at least 80% of the maximum. The isolated substorms and sawteeth reach their maximum F_{pc} close to onset, as expected. They also both have approximately the same temporal evolution. There appears to be slightly more of a growth phase, or storing of flux, before onset and a little more recovery phase after onset during the individual sawtooth. Since most sawtooth injections occur in a series the recovery phase of one

Table 1. Average polar cap open magnetic flux statistics for substorms and sawteeth.

Open magnetic flux in the polar cap (average)		
	Substorms	Sawteeth
Maximum (GWb)	0.68	1.07
Minimum (GWb)	0.47	0.74
Decrease (GWb)	0.21	0.33
% Decrease	30.8	30.4
Time for decrease (hours)	0.91	1.01
Rate of decrease (GWb/hour)	0.23	0.33

Table 2. The % of open flux released from the tail after onset for substorms and sawteeth.

% of open magnetic flux released (average)		
Minutes after onset	Substorms	Sawteeth
15	12.4	8.8
30	17.2	17.7
45	21.3	22.0
60	24.0	23.1

and the growth phase of the next must occur simultaneously and we see that superposition of the two effects.

For a more quantitative approach, we looked at the maximum and minimum fluxes of each type event and measured both the amount of change and the rate of change. The average released flux for isolated substorms is 0.21 GWb in an average of 54 min. For sawteeth there was an average decrease of 0.33 GWb in an average of 60 min. Giving the isolated substorms a rate of flux release is 0.0039 GWb /min and sawteeth 0.0055 GWb/min. However, if we look at the percent change from maximum to minimum, both individual sawteeth and isolated substorms drop by 30%. These measurements are listed in greater detail in Table 1.

The second approach uses the onset determined by LANL or magnetometer data. We look at the percent change in F_{pc} for 15, 30, 45, and 60 min past the onset. The results are shown in Table 2. As can be seen, there is very little difference between the two types of events. However, one of the problems with the method is the mismatch of onset times with the auroral onset.

For this portion of study we have left out the dayside boundary examined in the case studies. This is because for many of the events, especially when using UVI, the dayside boundary is not seen and has to interpolated. This process is fine for measuring the overall polar cap area and flux but not quite exact enough for an in-depth study. Because the IMF/solar wind parameters are so variable for sawteeth, (Huang et al., 2004) there was no real general pattern to be found in the data when placed into a superposed epoch and

Table A1. A List of SMCs used in the statistical study. Events were determined using the methodology set forth in DeJong and Clauer (2005). Start times are approximate and err on the side of cation, in that reconnection rates are balanced by the start time.

Steady magnetospheric convection events		
Date	Start time (UT)	Duration (hours)
10 Feb 1997	13:00	5.00
23 Feb 1997	02:00	5.00
5 May 1997	09:00	5.75
25 May 1997	00:00	4.25
19 June 1997	07:00	15.00
10 July 1997	14:50	9.00
9 Nov 1997	23:30	6.50
15 Nov 1997	05:30	4.50
10 Dec 1997	22:30	8.25
3 Feb 1998	16:00	9.00
14 Feb 1998	23:45	4.25
17 Feb 1998	14:45	8.50
19 Feb 1998	20:30	4.75
14 April 1998	08:00	4.50
20 April 1998	09:00	4.75
3 June 1998	21:00	3.75
14 June 1998	05:00	11.00
24 Sep 1998	05:00	4.00
4 Nov 1998	17:00	4.50
13 Jan 1999	02:00	9.00
28 April 1999	03:00	6.00
12 July 1999	11:00	7.00
8 Aug 1999	09:15	10.75
13 Aug 1999	14:30	5.50
23 Aug 1999	08:00	3.50
13 Nov 1999	01:30	3.50
14 Nov 1999	10:00	4.00
14 Nov 1999	14:30	3.50
23 Nov 1999	09:30	11.50
24 Jan 2000	16:00	4.25
10 March 2000	13:00	10.00
10 May 2000	03:00	17.00
21 Aug 2000	11:30	8.50
12 Sep 2000	13:30	6.00
30 Sep 2000	02:00	3.75
26 Oct 2000	03:00	4.00
20 Nov 2000	07:30	7.00
20 Nov 2000	16:00	4.50
22 Dec 2000	22:00	6.75
8 Jan 2001	17:00	3.50
15 Jan 2001	12:30	7.50
20 Jan 2001	16:00	3.00
21 Jan 2001	09:30	7.50
26 Jan 2001	04:00	3.50
12 May 2001	07:00	4.00
13 Nov 2001	18:00	3.50
16 Nov 2001	03:30	10.50

compared to substorms and SMCs. The only statement that can be made is the drivers appear to stronger for sawteeth

Table A2. A List of isolated substorms and individual sawteeth used in the statistical study. Only events with good auroral imaging were chosen. Onset times for the isolated substorms are determined by mid-latitude magnetometer data and onsets for the individual sawteeth are determined using LANL SOPA data (Cai et al., 2006a).

Isolated substorms		Individual sawteeth	
Date	Onset time (UT)	Date	Onset time (UT)
9 Jan 1997	07:47	11 Dec 1998	08:14
12 Sep 1997	19:58	19 Feb 1999	09:35
13 Sep 1998	07:26	16 Sep 1999	07:01
5 Dec 1997	07:17	16 Sep 1999	09:09
30 Dec 1997	05:25	16 Sep 1999	11:00
6 Jan 1998	02:48	11 Aug 2000	04:15
28 Feb 1998	04:50	11 Aug 2000	06:37
11 March 1998	08:12	11 Aug 2000	08:17
11 March 1998	22:52	11 Aug 2000	10:32
9 June 1998	08:01	7 Nov 2000	01:39
15 Sep 1998	06:40	7 Nov 2000	03:20
3 Dec 1998	07:07	29 Nov 2000	00:56
5 Dec 1998	07:13	29 Nov 2000	04:12
6 Oct 1999	08:06	21 Oct 2001	18:36
9 Oct 1999	05:05	21 Oct 2001	20:30
15 Jan 1999	04:43	21 Oct 2001	23:11
26 Jan 1999	09:59	22 Oct 2001	11:06
11 Feb 1999	00:32	22 Oct 2001	13:44
17 Feb 1999	16:39	18 April 2002	05:27
9 March 1999	04:30	18 April 2002	07:56
9 March 1999	18:00	18 April 2002	11:31
11 Nov 2000	17:41	18 April 2002	21:04
6 Dec 2000	15:17	19 April 2002	12:05
7 Dec 2000	21:51	19 April 2002	14:46
4 Jan 2001	06:47	20 April 2002	01:45
5 Dec 2001	08:58	20 April 2002	03:40
19 Dec 2001	01:29	20 April 2002	06:15
19 Dec 2001	10:19	3 Nov 2002	17:27
7 Jan 2002	09:15	21 Nov 2002	11:11
14 Jan 2002	12:32	–	–
16 Jan 2002	06:34	–	–

then substorms or SMCs, thus most likely causing a larger dayside merging rate for sawteeth than substorms. This is consistent with what described above.

5 Discussion

It appears that there are many similarities and differences when comparing these three types of events. The isolated substorms and SMCs studied here are similar in auroral intensity, extent of aurora in magnetic latitude, and amount of open magnetic flux. Whereas the individual sawtooth is larger in most respects than both the substorms and SMCs. Due to the on going debates about sawtooth injections and substorms (Cai et al., 2006a,b; Henderson et al., 2006) and

since we are only looking at one aspect of the events, we cannot yet say if an individual sawtooth is just a large substorm or something completely different. However, we can say that the amount of open magnetic flux released is larger for individual teeth, but the percentage released is the same as that of isolated substorms. It also appears that the auroral oval, during the individual teeth, extends further into the inner magnetosphere than isolated substorms or SMCs, based on the auroral equatorward edge. In order to more fully explore the differences of these events, more data will need to be studied and more events will need to be investigated in the IMAGE FUV and Polar UVI data.

References

Baker, J. B., Clauer, C. R., Ridley, A. J., Papitashvili, V. O., Brittnacher, M. J., and Newell, P. T.: The nightside polarward boundary of the auroral oval as seen by DMSP and the Ultraviolet Imager, J. Geophys. Res, 105, 21 267–23 280, 2000.

Borovsky, J. E.: Global Sawtooth Oscillations of the Magnetosphere, Eos Trans. AGU, Fall Meeting Suppl., Abstract SM23B-04, 2004.

Brittnacher, M., Fillingim, M., Parks, G., Germany, G., and Spann, J.: Polar cap area and boundary motion during substorms, J. Geophys. Res., 104(A6), 12 251–12 262, 1999.

Cai, X., Clauer, C. R., and Ridley, A. J.: Statistical analysis of ionospheric potential patterns for isolated substorms and sawtooth events, Ann. Geophys., 24, 1977–1991, 2006a.

Cai, X., Henderson, M. G., and Clauer, C. R.: A statistical study of magnetic dipolarization for sawtooth events and isolated substorms at geosynchronous orbit with GOES data, Ann. Geophys., 24, 3481–3490, 2006b.

Clauer, C. R. and McPherron, R.: Mapping the local time-universal time development of magnetospheric substorms using mid-latitude magnetic observations, J. Geophys. Res., 79, 2811–2820, 1974.

Cowley, S. W. H. and Lockwood, M.: Excitation and decay of solar wind-driven flow in the magnetophere-ionosphere system, Ann. Geophys., 10, 103–115, 1992,
http://www.ann-geophys.net/10/103/1992/.

DeJong, A. D. and Clauer C. R.: Polar UVI Images to Study Steady Magnetospheric Convection Events: Initial Results, Geophys. Res. Lett., 32, L24101, doi:10.1029/2005GL024498, 2005.

Fillingim, M. O., Parks, G. K., Chen, L. J., Brittenacher, M., Germany, G. A., Spann, J. F., Larson, D., and Lin, R. P.: Coincident POLAR/UVI and WIND observations of pseudobreakups, Geophys. Res. Lett., 27, 1379–1382, 2000.

Henderson, M. G., Reeves, G. D., Skoug, R., Thomsen, M. F., Denton, M. H., Mende, S. B., Immel, T. J., Brandt, P. C., and Singer, H. J.: Mangetospheric and auroral activity during the

18 April 2002 sawtooth event, J. Geophys. Res., 111, A01S90, doi:10.1029/2005JA011111, 2006.

Huang, C. S., Le, G., and Reeves, G.: Periodic magnetospheric substorms during fluctuating interplanetary magnetic field B_z, Geophys. Res. Lett., 31, L14801, doi:10.1029/2004GL020180, 2004.

Immel, T. J., Craven, J. D., and Nicholas, A. C.: An empirical model of the OI FUV dayglow from DE-1 images, J. Atmos. Solar-Terr. Phys., 62, 47–64, 2000.

Kamide, K., Kokubun, S., Bargatze, L. F., and Frank, L. A.: The size of the polar cap as an indicator of substorm energy, Phys. Chem. Earth, 24, 119–127, 1999.

Koshkinen, H. E. J., Lopes, R. E., Pellinen, R. J., Pulkkinen, T. I., Baker, D. N., and Bosinger, T.: Pseudobreakup and Substorm Growth Phase in the Ionosphere and Magnetosphere, J. Geophys. Res., 98(A4), 5801–5813, 1993.

Milan, S. E., Lester, M., Cowley, S. W. H., Oksavik, K., Brittnacker, M., Greenwald, R. A., Sofko, G., and Villain, J. P.: Variations in the polar cap area during two substorm cycles, Ann. Geophys., 21, 1121–1140, 2003,
http://www.ann-geophys.net/21/1121/2003/.

Milan, S. E.: A simple model of the flux content of the distant magnetotail, J. Geophys. Res., 109, A07210, doi:10.1029/2004JA010397, 2004.

Milan, S. E., Wild, J. A., Grocott, A., and Draper, N. C.: Space- and ground-based investigations of solar wind-magntosphere-ionosphere coupling, Adv. Space Res., 38, 1671–1677, 2006.

O'Brien, T. P., Thompson, S. M., and McPherron, R. L.: Steady magnetospheric convection: Statistical signatures in the solar wind and AE, Geophys. Res. Lett., 29, 23, doi:10:1029/2001GL019113, 2002.

Perraut, S., Le Contel, O., Roux, A., Parks, G., Chua, D., Hoshino, M., Mukai, T., and Nagai, T.: Substorm expansion phase: Observations from Geotail, Polar and IMAGE network, J. Geophys. Res., 108(A4), 1159, doi:10.1029/2002JA009376, 2003.

Sergeev, V. A., Kubyshkina, M. V., Liou, K., Newell, P. T., Parks, G., Nakamura, R., and Mukai, T.: Substorms and convection bay compared: auroral and magnetotial dynamics during convection bay, J. Geophys. Rev., 106(A9), 18 843–18 855, 2001.

Sergeev, V. A., Pellinen, R. J., and Pulkkinen, T. I.: Steady magnetospheric convection: a review of recent results, Space Sci. Rev., 75, 551–604, 1996.

Siscoe, G. L. and Huang, T. S.: Polar cap inflation and deflation, J. Geophys. Rev., 90(A1), 543–547, 1985.

Weimer, D. R., Ober, D. M., Maynard, N. C., Burke, W. J., Collier, M. R., McComas, D. J., Ness, N. F., and Smith, C. W.: Variable time delays in the propagation of the interplanetary magnetic field, J. Geophys. Res., 108(A1), 16, 1026–1034, doi:10.1029/2002JA009405, 2003.

Weimer, D. R., Ober, D. M., Maynard, N. C., Burke, W. J., Collier, M. R., McComas, D. J., Ness, N. F., Smith, C. W., and Watermann, J.: Predicting interplanetary magnetic field (IMF) propagation delays times using minimum variance technique, J. Geophys. Res., 107(A8), 29, 1210–1222, doi:10.1029/2001JA009102, 2002.

Weimer, D. R.: Correction to "Predicting interplanetary magnetic field (IMF) propagation delays times using minimum variance technique", J. Geophys. Res., 109, A12104, doi:10.1029/2004A010691, 2004.

Yahnin, A., Malkov, M. V., Sergeev, V. A., Pellinen, R. J., Aulamo, O., Vennerstrom, S., Friis-Christensen, E., Lassen, K., Danielsen, C., Craven, J. D., Deehr, C., and Frank, L. A.: Features of steady magnetospheric convection, J. Geophys. Res., 99(A3), 4039–4051, 1994.